IOP Publishing Plasma Sources Science and Technology

Plasma Sources Sci. Technol. **23** (2014) 065047 (9pp) doi:10.1088/0963-0252/23/6/065047

Self-organization of single filaments and diffusive plasmas during a single pulse in dielectric-barrier discharges

Natalia Yu Babaeva[1] **and Mark J Kushner**[2]

Department of Electrical Engineering and Computer Science, University of Michigan, 1301 Beal Ave, Ann Arbor, MI 48109-2122, USA

E-mail: nbabaeva@umich.edu, nbabaeva@ihed.ras.ru and mjkush@umich.edu

Received 16 June 2014, revised 10 August 2014
Accepted for publication 2 October 2014
Published 11 November 2014

Abstract

Self-organization of filaments in dielectric-barrier discharges (DBDs) probably has many origins. However, the dominant cause is proposed to be the accumulation of charge on the surfaces of the bounding dielectrics that reinforces successive discharge pulses to occur at the same locations. A secondary cause is the electrostatic repulsion of individual plasma filaments. Self-organization typically develops over many discharge pulses. In this paper, we discuss the results of a computational investigation of plasma filaments in overvoltage DBDs that, under select conditions, display self-organized patterns (SOPs) of plasma density during a single discharge pulse. (Overvoltage refers to the rapid application of a voltage in excess of the quasi-dc breakdown voltage.) The origin of the SOPs is a synergistic relationship between the speed of the surface-ionization waves that propagate along each dielectric and the rate at which avalanche occurs across the gap. For our test conditions, SOPs were not observed at lower voltages and gradually formed at higher voltages. The same conditions that result in SOPs, i.e. the application of an overvoltage, also produce more diffuse discharges. A transition from a single narrow filament to a more diffuse structure was observed as overvoltage was approached. The sensitivity of SOPs to the orientation and permittivity of the bounding dielectrics is discussed.

Keywords: self-organized, dielectric-barrier discharge, diffuse atmospheric pressure discharge

(Some figures may appear in colour only in the online journal)

1. Introduction

Dielectric-barrier discharges (DBDs) are formed by applying an alternating high voltage across two electrodes where at least one of the electrodes is covered by a dielectric [1]. The high electric field so produced creates a discharge that, in the absence of the dielectric, would rapidly progress to an arc. Arc formation is prevented by accumulating charge on the dielectric surface, which charges the capacitance of the dielectric and removes voltage from the gas gap. This reduction in voltage limits the current and prevents an uncontrolled discharge from developing. With sufficient charging of the dielectric, the discharge can no longer be sustained and extinguishes. When the voltage changes sign with each half-cycle of the applied voltage, breakdown may be reinforced at the same location due to the previous charging of the dielectric. A typical filament in a DBD may be a few hundred micrometers in diameter and last about 10 ns.

The accumulation of charges on the dielectric not only reduces the voltage drop across each plasma filament to prevent arcing, but can also lead to self-organization of the filaments, which produces a variety of quasi-static patterns. Pattern formation in DBDs has been expressed as self-organized patterns (SOPs) which include hexagons, stripes, spirals, bands and concentric rings [2–18]. Pattern formation is often explained by a memory effect. The charging of the

[1] Now with the Joint Institute for High Temperatures Russian Academy of Sciences, Izhorskaya 13, Moscow 125412, Russian Federation.
[2] Author to whom any correspondence should be addressed.

dielectric that extinguishes the filament on one half-cycle of bias by reducing voltage across the gap will initially add to the voltage on the next half-cycle. This local increase in voltage increases the likelihood that a filament will be produced at the same location on the second half-cycle. Another cause of pattern formation of plasma filaments is mutual electrostatic interaction between the filaments. The filaments in a DBD are a form of streamer that propagates by space charge separation in the head of the streamer. Streamers that are sufficiently close will feel the repelling electrostatic force of neighboring filaments. The most stable of such arrangements of many plasma filaments is hexagonal spacing. The spreading of the discharge on the dielectric surfaces can also contribute to an electrostatically based spacing of the filaments.

Guikema *et al* [7] observed three types of periodic patterns of filaments in DBDs, as well as a disordered state in which filaments form at apparently random positions and times. At relatively low voltages, the patterns consisted of narrow filaments with relatively wide separation. With an increase in voltage, the spacing of the filaments decreased until at sufficiently high voltage, the filaments were produced in what appeared to be random locations. Shirafuji *et al* [4] investigated symmetric self-organized filaments in a radio frequency DBD sustained in Ar between parallel quartz plates with MgO films. They found the need for an attractive force, in addition to the Lorentz force of parallel wires, to offset the electrostatic repulsion between filaments in order to confine the small number of self-organized filaments in their experiment. Dong *et al* [2, 8, 9, 11] have observed a variety of patterns of filaments, including spirals and hexagonal and square lattices. Interlacing super lattice patterns have also been observed. Ar and Ar/air mixtures were investigated with planar glass plates as dielectric barriers and water electrodes. They found a correlation of the temporal dynamics of individual filaments with the change of the spatial symmetry of the filament patterns as the applied voltage increased, as well as collective vibration of the SOP [11].

Stollenwerk [12] found that otherwise stable filament patterns in DBDs will spontaneously begin to move. The filaments will occasionally collide and annihilate each other. The annihilation appears to take place before the filaments visibly touch each other. Using experiments and models, Bernecker *et al* [13] observed a new form of self-organization in which filaments produce interlaced patterns that shift half a spatial period every half-cycle. Boeuf *et al* [14] demonstrated the growth (from half-cycle to half-cycle) of side discharges around an isolated filament until the side discharge itself becomes a full filament. Patterns can therefore quickly form around an initial filament or local perturbation. Isolated filaments are observed in this regime and can merge when the distance between them is below a critical value.

Zhang and Kortshagen modeled a DBD operating in He with a small N_2 impurity (20 ppm) over many sinusoidal cycles (10–25 kHz) and found different regimes of uniformity or self-organization [15]. They found that filamentary discharges with periodic self-organization were produced at lower frequencies and with dielectrics having larger permittivity. When increasing frequency, sufficient pre-ionization remained from the previous discharge to seed a uniform plasma.

Most proposals for the causes of self-organization rely to some degree on the accumulation of surface charges or interactions between plasma filaments over many discharge cycles. This trend is well demonstrated in pulse-to-pulse experimental measurements of optical emission and three-dimensional (3D) modeling dielectric charging by Stollenwerk *et al* [16], and in 3D simulations by Bhoj and Kolobov [17]. In this paper, we report on the results of a computational investigation in which evidence for self-organization is found during a single discharge pulse sustained in humid air. These observations are for DBDs sustained in air at atmospheric pressure over a range of voltages. We found that at low voltage, a single filament is formed with nominal spreading of the discharge on the surface of the dielectrics. With higher voltage, there is a transition to a more diffuse, but still uniform discharge. With successively higher voltages, low intensity, periodic ionization waves are launched from the tips of the spreading discharge on the dielectric. The shapes and propensity to form these periodic structures depend on the relative capacitances of the top and bottom dielectrics, which determine the rate of spreading of the surface-ionization waves (SIWs). The discharges we investigated are for overvoltage conditions. For these conditions the high rate of voltage rise enables the applied voltage to significantly exceed the quasi-static breakdown voltage of $30\,\mathrm{kV\,cm^{-1}}$. This overvoltage condition contributes to the more diffuse nature of the discharges.

The model used in this investigation is described in section 2. Single pulse self-organization resulting from an individual filament in a DBD is discussed in section 3. Our concluding remarks are made in section 4.

2. Description of the model and geometry

The model used in the investigation, *nonPDPSIM*, is a two-dimensional simulator in which Poisson's equation for the electric potential, and transport equations for charged and neutral species, are solved. The model is discussed in detail in [18, 19] and so is only briefly described here. Charged particle transport is addressed using a fully implicit algorithm coincident with solving Poisson's equation for the electric potential. Poisson's equation is solved throughout the entire computational domain, including the gas phase and solid dielectrics. Charge accumulation is accounted for on the surface of dielectrics. The electron temperature is obtained by solving an electron energy conservation equation with transport and rate coefficients coming from local solutions of Boltzmann's equation. Radiation transport and photoionization are included by implementing a Green's function propagator. The gas phase reaction mechanism for 1 atm of humid air ($N_2/O_2/H_2O = 79/20/1$) and other computational algorithms are the same as those described in [19]. The humidity impacts the calculation due to water's effect on the transport coefficients, ionization and dissociation (including dissociative attachment) of H_2O, and neutralization reactions between negative ions and H_2O^+. Due to the calculation extending only to 25 ns, the higher order water cluster ions were not included.

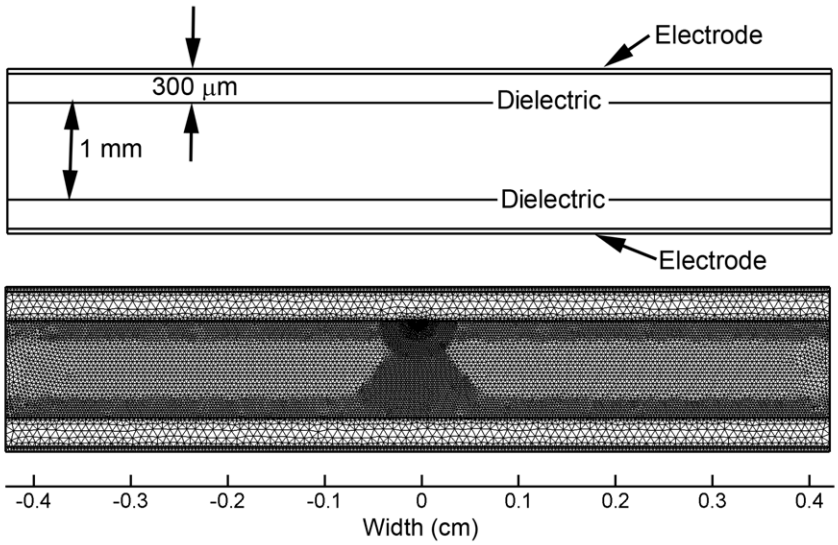

Figure 1. Geometry used in the model. (top) The 1 mm gap is bounded by 300 μm thick dielectric plates which are backed by metal electrodes. The top electrode is biased and the bottom is grounded. (*b*) The computational mesh is highly refined where the initial filament occurs and where the SIWs propagate.

The geometry used in the model is shown in figure 1. The computational domain is 8.5 mm $\times$ 1.7 mm. The numerical grid uses an unstructured mesh with triangular elements. The gas gap is 1 mm and is bounded by dielectric plates 0.3 mm thick whose relative permittivity, $\varepsilon_r = \varepsilon/\varepsilon_0$, is varied. Each plate is bounded by a planar metal electrode. The top electrode is powered and the lower electrode is grounded. The mesh consists of approximately 12 500 nodes, of which about 8900 are in the plasma region. Mesh spacing near surfaces and in the primary streamer region is about 25 μm. The lateral boundaries are dielectric surfaces which effectively implement Neumann boundary conditions for the electric potential.

The plasma is initiated by artificially emitting electrons from three mesh points with a total current density of about 10 A cm^{-2} at the surface and in the middle of the top dielectric. The plasma otherwise sustains itself through volumetric ionization and secondary processes. The secondary electron emission coefficient is 0.2 for all ions and 0.01 for photons.

3. SOPs produced by a single plasma filament

The propagation and spreading of plasma for a single DBD filament for a step function voltage of -10 kV are shown in figure 2. (The voltage rise time is 0.1 ns and is then held constant for the duration of the calculation.) The electron density, rate of electron impact ionization, rate of photoionization and electric potential are sequentially shown in time. (The notation in the figures, for example, 3-decade, means that the minimum value plotted is 10^{-3} of the maximum value plotted.) The permittivity is $\varepsilon_r = 30$ for the top dielectric and $\varepsilon_r = 3$ for the bottom. The choice of these dielectric constants results in the capacitance of the top dielectric exceeding that of the lower dielectric. The plasma filament crosses the 1 mm gas gap in about 1.2 ns. Upon intersection of the filament with the lower dielectric surface, the more mobile electrons charge the surface of the lower dielectric, which traps electric potential lines in the dielectric. This in turn removes voltage from the gap at that location and reduces the electric field in the gap. This is, in fact, the fundamental mechanism whereby DBDs limit current and prevent arcing.

Since this is negative discharge, the more mobile electrons are accelerated into the surface of the lower dielectric. In charging the dielectric, lateral components of the electric field are produced, which then initiates an outwardly propagating SIW. The SIW is in part sustained by the electric field enhancement that occurs at the surface of the dielectric between the region of charged and uncharged surface. The curvature of the electric potential contours produced by the charging of the surface and the discontinuity in permittivity enhances the electric field to help sustain the SIW. A positive ionization wave is launched from the region of high electric field at the edge of the SIW. This positive ionization wave sweeps radially outward with the propagation of the SIW. This occurs at a time when there is a weak background photoionization that seeds the SIW. Once the voltage has collapsed due to surface charging behind the SIW, the photoionization from long-living excited states is the dominant source of ionization. The ionization source at the top dielectric is in large part sustained by photoelectron emission that produces electrons in the cathode-fall-like boundary layer.

The space charge residing on the surface of the upper dielectric results in a cathode-fall-like sheath that forms at the cathode-acting dielectric. This produces a positive SIW. When the capacitances of the top and bottom dielectrics are the same, the speed of the top SIW is higher than that for the negative SIW on the bottom dielectric. In order to approximately equilibrate the speeds of the SIWs on the top and bottom surfaces, we chose different dielectric constants for the top and bottom dielectrics. The larger capacitance (F cm^{-2}) of the top dielectric requires a longer dwell time to charge the capacitance and so reduces the speed of what would have been the faster SIW.

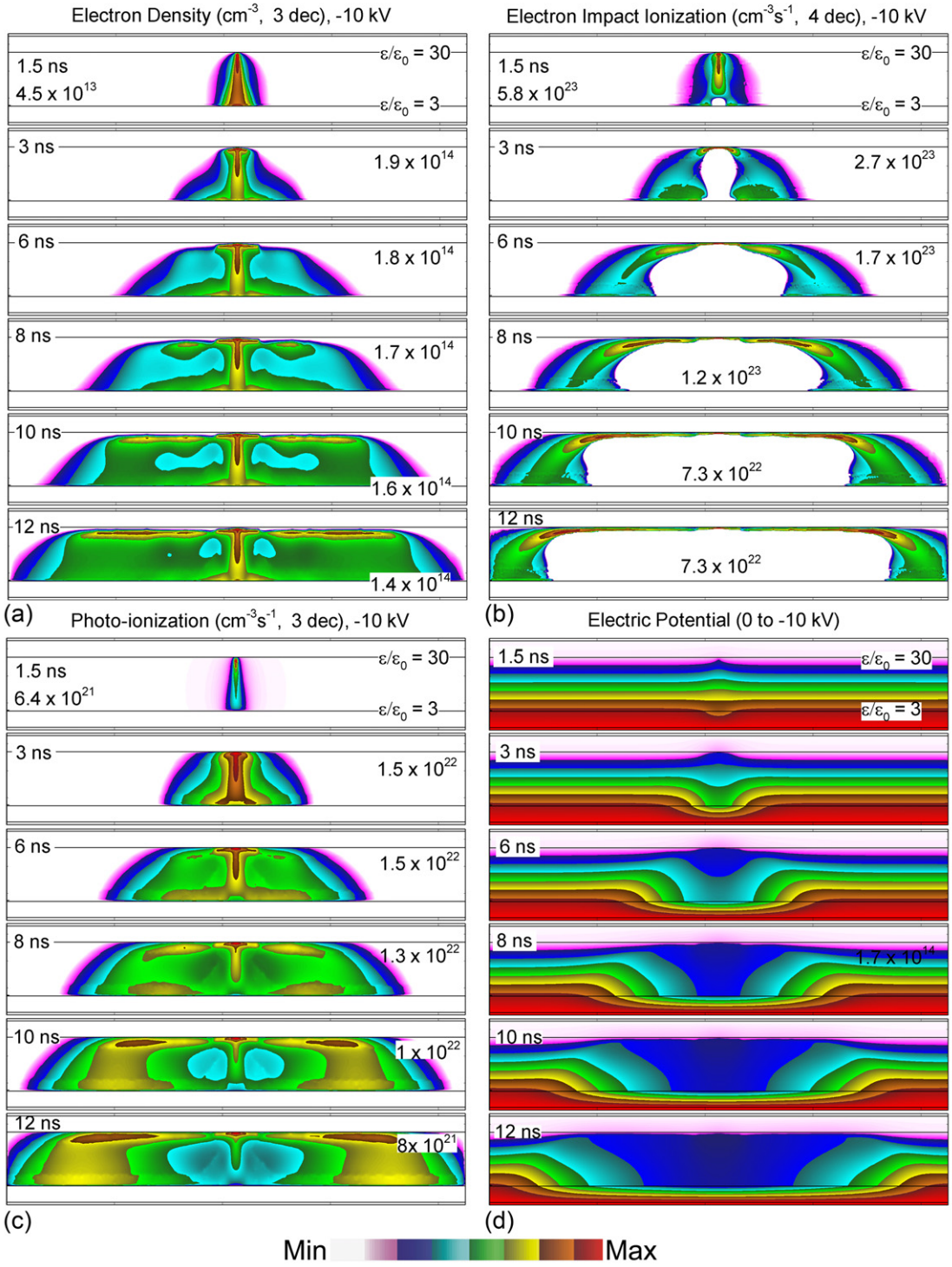

Figure 2. Plasma properties for a single discharge pulse for different times after application of −10 kV bias. (*a*) Electron density (cm^{-3}), (*b*) electron impact ionization rate ($cm^{-3}\ s^{-1}$), (*c*) photoionization rate ($cm^{-3}\ s^{-1}$), and (*d*) electric potential (kV). The top dielectric has $\varepsilon_r = 30$ and the lower dielectric has $\varepsilon_r = 3$. The maximum value plotted is noted in each frame, as is the number of decades plotted for log plots. The expanding SIWs initiate ionization in the gap which produces a fairly diffuse plasma.

The end result is that after the SIW has traversed the 0.5 cm on either side of the primary filament and encountered the bounding dielectrics, a diffuse electron density remains. At 12 ns, the electron density at mid-gap is about $2.2 \times 10^{13}\ cm^{-3}$ and is produced by the propagation of the initial DBD filament. The background electron density trailing the SIW is $3 \times 10^{12}\ cm^{-3}$ and is locally uniform to about 10%. This is an example of a diffuse-like discharge resulting from overvoltage, as discussed in more detail below.

Electron densities at different times for an applied voltage of −20 kV for conditions that are otherwise the same are shown in figure 3. The sequence of events for filling the gap with plasma is basically the same as for the −10 kV case—albeit accelerated by nearly an order of magnitude in time due to

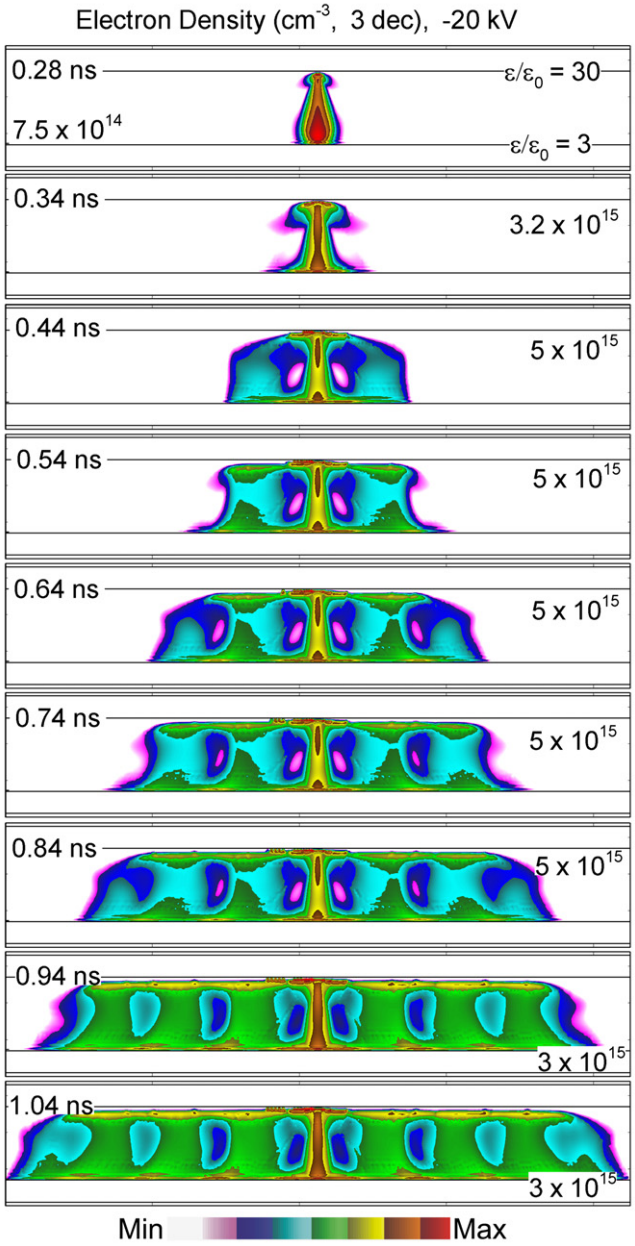

Figure 3. Electron density (cm^{-3}) for a single discharge pulse for different times after application of a -20 kV bias. The top dielectric has $\varepsilon_r = 30$ and the lower dielectric has $\varepsilon_r = 3$. The maximum value plotted is noted in each frame for three-decade log plots. The expanding SIWs initiate a periodic ionization wave through the gap that produces a SOP.

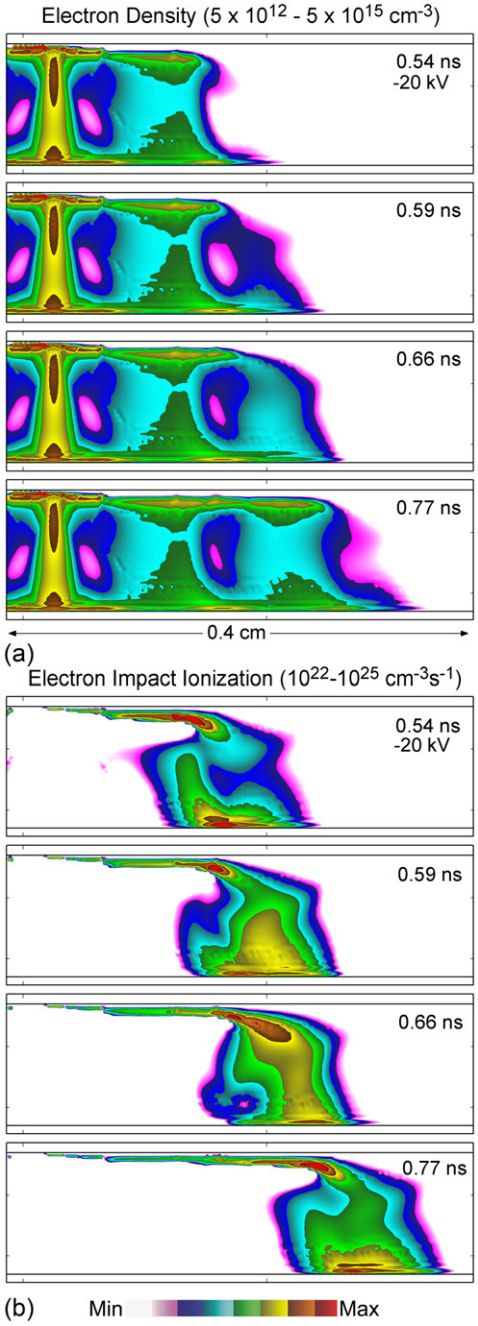

Figure 4. Processes leading to formation of a SOP for a bias voltage of -20 kV. (*a*) Electron density (cm^{-3}) and (*b*) electron impact ionization rates ($cm^{-3}\,s^{-1}$). The images are three-decade log plots. Positive ionization waves are launched from the edge of the expanding SIW on the lower dielectric and rapidly cross the gap to meet the SIW on the upper dielectric.

the higher applied voltage. Although qualitatively similar, the details of the spreading of the plasma are different. As the SIWs expand on both electrodes in both directions, the plasma in the gap is produced in a periodic pattern. In this case, the period of electron density is 900–950 μm. The sequence of events that generates this pattern is shown in figure 4, where the electron density and rate of electron impact ionization are shown for the second period. After formation of the previous period at 0.54 ns (in this case, the first period is to the right of the primary filament), the voltage across the gap has been reduced to below the avalanche level. However, there is sufficient lateral electric field to maintain the SIW along the lower dielectric. The SIW proceeds about 700–800 μm without there being significant ionization in the volume (0.59 ns). This leaves a hole (a local minimum) in the electron density in the gap. As the SIW continues to proceed outwards, the voltage across the gap increases due to the lower conductivity of the plasma in the gap, and due to there being less surface charging. The voltage and E/N (electric field/gas density) in the gap increase to the point that an ionization wave is launched into the gap (0.66 ns) from the edge of the SIW where

the electric field is enhanced (see, for example, figure 2(*d*)). The ionization wave is positive and upwardly directed. This positive ionization wave connects the bottom and top SIWs by conductive plasma, which in turn charges the dielectrics and turns off the volumetric ionization wave (0.77 ns). At this point, the second period ends. The process repeats itself, resulting in a SOP on a single discharge pulse.

There is a threshold voltage for both significant lateral propagation of the SIWs and for producing the periodic ionization waves that generate the periodic pattern of electron density. For example, the electron density is shown in figure 5(*a*) for applied voltages of −6.25 to −20 kV. Electron densities in the middle of the gap for a subset of these voltages normalized by the maximum electron density in the central filament are shown in figure 6. The maximum electron density increases from 1.5×10^{13} cm^{-3} at −6.25 kV to 3×10^{15} cm^{-3} at −20 kV. For magnitudes of voltages less than −8.75 kV, the SIWs do not significantly propagate and the plasma does not spread beyond the initial filament. At −8.75 kV the plasma begins to spread on the lower dielectric with the smaller permittivity; however, the SIW fails to propagate along the top dielectric. At this voltage, the larger capacitance of the top dielectric requires additional current to charge, and so slows the propagation of the SIW. For discharges from −10 kV, the SIWs do propagate on both dielectric surfaces, spreading the plasma well beyond the initial filament. This onset of a more extensive region of ionization occurring between −8.75 kV and −20 kV is a diffuse mode of operation, as opposed to a single, isolated filamentary mode.

In spite of the diffuse mode beginning at −10 kV, the SOP does not occur for −10 kV. There is a range of voltages which produces a broader, more diffuse mode plasma but does not produce a SOP. At −12.5 kV, the SOP begins to form with an amplitude that decays as the SIWs propagate outward. Here, the voltage drop along the surface of the dielectrics as the SIWs propagate reduces the voltage available to launch the abrupt positive ionization waves across the gap. The SOP therefore dies out. At −15 kV, the SOP pattern deepens and the SIWs propagate further laterally before the SOP decays. For −20 kV, the SOP extends to the boundary of the computational domain and would have continued beyond the extent shown for a larger computational domain. This is the case to some extent for all the cases investigated with the exception of lower voltages that do not sustain SIWs.

The formation of the SOP results from a balance between the rate of propagation of the SIWs which extend the region of electric field enhancement to greater distances, the seeding of plasma by photoionization and the rate of avalanche in the volume. In the −7.5 kV case, the voltage remaining after closing the gap is insufficient to support propagation of SIWs. The large lateral extent of the SIWs requires overvoltage which, for these conditions, begins with −10 kV. In the −10 kV case, the propagation of the SIWs and the rate of avalanche in the volume are in quasi-equilibrium, which produces a fairly uniform and diffuse bulk plasma. In the −20 kV case, the speed of propagation and the rate of avalanche are both about an order of magnitude higher than at −10 kV. The speed of the SIW extends the region of electric field enhancement at the surface beyond the edge of the plasma in the gap into a region of higher E/N. The rate of avalanche across the gap is then sufficiently rapid that the plasma is formed while the SIW is nearly stationary.

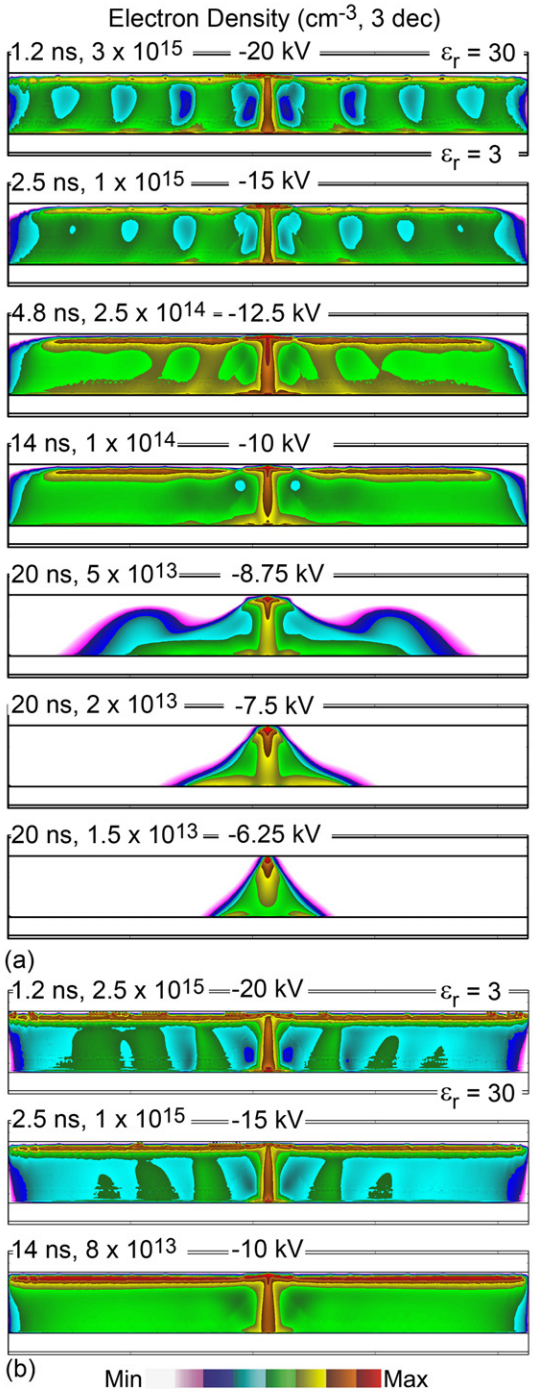

Figure 5. Electron density (cm^{-3}) for different voltages and permittivities. (*a*) Electron density (three-decade log scale) for applied voltages of −6.25 kV to −20 kV for $\varepsilon_r = 30$ on the top dielectric and $\varepsilon_r = 3$ on the bottom dielectric. (*b*) Electron density (three-decade log scale) for −10 kV, −15 kV and −20 kV applied voltage for $\varepsilon_r = 3$ on the top dielectric and $\varepsilon_r = 30$ on the bottom dielectric.

The pattern formation also depends on the relative speeds of the SIWs on the top (cathode-like) and bottom (anode-like)

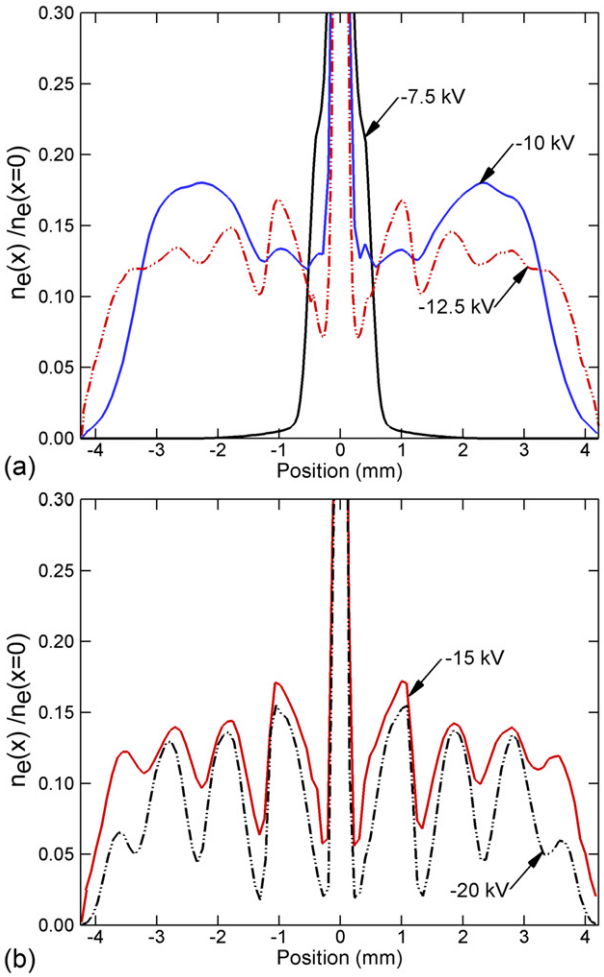

Figure 6. Electron density at mid-gap normalized by the maximum electron density in the filament for applied voltages of (*a*) −7.5 kV, −10 kV and −12.5 kV, and (*b*) −15 kV and −20 kV. The lowest voltage, −7.5 kV, does not sustain lateral propagation of SIWs during 20 ns. As voltage increases, the discharge spreads and a SOP forms at −12.5 kV.

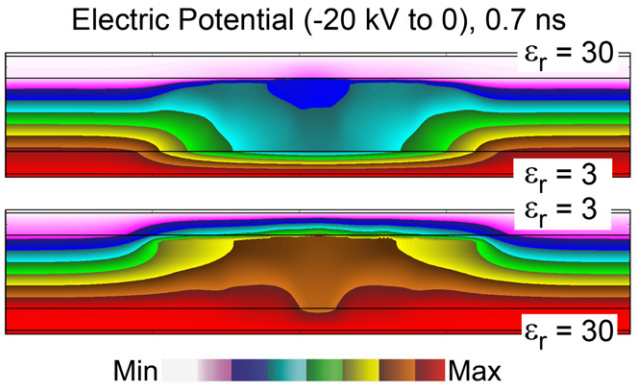

Figure 7. Electric potential (kV) for −20 kV with (top) $\varepsilon_r = 30$ and 3 on the top and bottom electrodes, compared to (bottom) $\varepsilon_r = 3$ and 30 on the top and bottom electrodes.

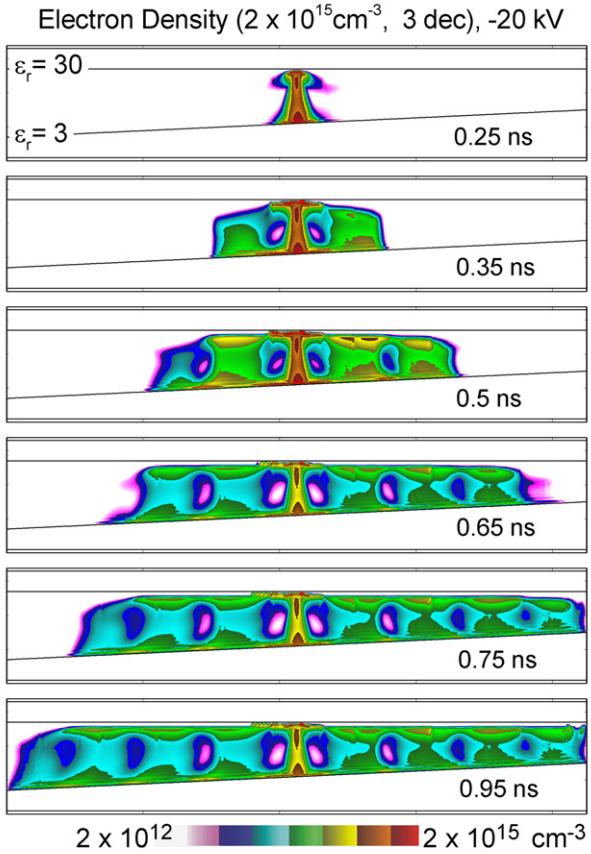

Figure 8. Electron density (cm^{-3}) (three-decade log plot) for a single discharge pulse for different times after application of −20 kV bias with a tilted bottom dielectric. The top dielectric has $\varepsilon_r = 30$ and the lower dielectric has $\varepsilon_r = 3$. The SIWs propagate more rapidly into the narrowing gap and form more discrete SOPs compared to the plasma in the widening gap.

dielectrics. These speeds can be controlled by the permittivity of the respective dielectrics. For example, the electron density is shown in figure 5(*b*) for $\varepsilon_r = 3$ on the top electrode and $\varepsilon_r = 30$ on the bottom electrode, the opposite of the prior cases. The propensity for producing the SOP is diminished. The SOP initially forms and then decays away after two or three periods. With the change in capacitance (now larger on the bottom) the SIW propagates more slowly on the bottom dielectric than on the top, as shown by the electric potential in figure 7. The surface intensified electric field is now largest at the top surface but weaker than in the base case. As the SIW on the top surface propagates farther from the primary filament, the electric field enhancement weakens and so the ability to launch ionization waves into the volume decreases. Note that in the base case, the ionization waves through the gap are vertically directed or perhaps bent a bit inward and are positive ionization waves. When changing the permittivities to have the more rapid SIW on the top surface, the ionization waves through the gap are bent outwards and are negative ionization waves.

In applications of DBDs such as plasma medicine, the spacing between the powered electrode in the applicator and the surface to be treated may not be uniform due to tilting of either the applicator or the surface being treated. The sensitivity of the alignment of the electrodes is demonstrated by the electron density shown in figure 8. Here we have $\varepsilon_r = 30$ on the top electrode and $\varepsilon_r = 3$ on the bottom electrode as in the base case. The lower dielectric slopes upward to the right at an angle of 2.8° (1.26 mm gap on the far left and 0.74 mm on the

far right). After the initial filament is formed, SIWs propagate in both directions as with flat dielectrics. The qualitative behavior of the SOP is the same for the SIW propagating into both the narrowing and widening gaps. However, the SIWs propagate more rapidly and the SOPs are more clearly defined in the narrowing gap compared to the widening gap. Due to the slope of the dielectric, there is about a 20% increase in initial E/N from the left (widening) to right (narrowing) sides of the gap, and this increase in E/N will produce faster SIWs and more clearly defined SOPs. There is also a decrease in capacitance to the right due to the thickening dielectric as the gap narrows. This decrease in capacitance will increase the propagation speed of the SIW in the narrowing gap.

The overvoltage that produces SOPs also contributes to more diffuse and extended filaments in DBDs. The correlation between diffusive-appearing DBDs and the rate of voltage rise has recently been noted by Hirschberg *et al* [20], Yang *et al* [21] and Liu *et al* [22]. For example, Liu *et al* [22] quantified the transition from a filamentary to a diffuse mode in DBDs sustained in air when applying a larger overvoltage. Applying the overvoltage typically requires a fast-rising voltage pulse. When imaging single DBD pulses (20 ns exposure) in atmospheric air, Liu *et al* observed a transition from a discharge composed of isolated filaments with an applied electric field of 54.8 kV cm^{-1} or 211 Td (21.9 kV, 4 mm gap) to a diffuse plasma for an electric field of 185 kV cm^{-1} or 711 Td (18.4 kV, 1 mm gap). In our simulations, we interpret the onset of a diffuse mode when the SIWs extend the single plasma filament in the center of the dielectric plates to significantly greater widths. The wider plasma has a lower plasma density than the central filament, which would be consistent with experimental imaging [22]. The threshold for forming diffuse discharges was measured by Liu *et al* to be about 120 kV cm^{-1} or 462 Td [22]. Our simulations of single pulses predict a diffuse-like mode beginning between -8.75 kV and -10 kV, or between 87.5 and 100 kV cm^{-1}.

4. Concluding remarks

The formation of SOPs in DBDs resulting from a single filament and a single discharge pulse was discussed with results from a two-dimensional computer model for discharges sustained in humid air. We found that SOPs may form under select conditions of overvoltage. The SOPs are formed by a periodic avalanching of the gap while SIWs on the top and bottom dielectrics propagate outward from the initial filament. The formation of the SOPs is sensitive to the relative speeds of the SIWs on the top and bottom dielectrics, and to the rate at which avalanche of the gas gap occurs. Electric field enhancement at the edge of the SIW provides the means to launch the ionization waves that form the periodic pattern into the gap. To form SOPs, the rate of avalanche across the gap should be rapid compared to the speed of expansion of the SIWs. For the conditions investigated, 1 atm of humid air, higher voltages produced more diffusive discharges which also have clearer SOPs. The formation of SOPs by this mechanism in humid air benefits from the sharp demarcation between attachment-dominated and ionization-dominated transport as a function of E/N. Over a small range of E/N, electron transport transitions from being highly attaching to being avalanching, conditions that enable quick turn-on of the ionization wave launched from the SIW into the gap. We expect that most gas mixtures that have such a sharp demarcation between attachment and avalanche will produce SOPs. For example, simulations show that similar SOPs are produced in dry air. As this demarcation becomes less sharp, the SOPs will likely become less clear and eventually dissipate. The conditions which produce more diffusive discharges correlate well with experimental observations of diffuse discharges in DBDs occurring with significant overvoltage.

Acknowledgments

This work was supported by the United States Department of Energy Office of Fusion Energy Science (DE-SC0001319) and the National Science Foundation (CHE-1124724).

References

[1] Kogelschatz U 2003 Dielectric-barrier discharges: their history, discharge physics, and industrial applications *Plasma Chem. Plasma Process* **23** 1
[2] Dong L F, Xiao H, Fan W L, Yin Z Q and Zhao H T 2010 Temporal symmetry of individual filaments in different spatial symmetry filaments pattern in a dielectric barrier discharge *Phys. Plasmas* **17** 102314
[3] Müller L, Punset C, Ammelt E, Purwins H-G and Boeuf J P 1999 Self-organized filaments in dielectric barrier glow discharges *IEEE Trans. Plasma Sci.* **27** 20
[4] Shirafuji T, Kitagawa T, Wakai T and Tachibana K 2003 Observations of self-organized filaments in a dielectric barrier discharge of Ar gas *Appl. Phys. Lett.* **83** 2309
[5] Gurevich E L, Zanin A L, Moskalenko A S and Purwins H-G 2003 Concentric-ring patterns in a dielectric barrier discharge system *Phys. Rev. Lett.* **91** 154501
[6] Chirokov A, Gutsol A, Fridman A, Sieber K D, Grace J M and Robinson K S 2006 A study of two-dimensional microdischarge pattern formation in dielectric barrier discharges *Plasma Chem. Plasma Process* **26** 127
[7] Guikema J, Miller N, Niehof J, Klein M and Walhout M 2000 Spontaneous pattern formation in an effectively one-dimensional dielectric-barrier discharge system *Phys. Rev. Lett.* **85** 3817
[8] Dong L, Fan W, He Y and Liu F 2008 Self-organized gas-discharge patterns in a dielectric-barrier discharge system *IEEE Trans. Plasma Sci.* **36** 1356
[9] Dong L, Yin Z, Li X, Chai Z and He Y 2006 Spatio-temporal patterns in dielectric barrier discharge in air/argon at atmospheric pressure *Plasma Sources Sci. Technol.* **15** 840
[10] Stauss S, Muneoka H, Ebato N, Oshima F, Pai D Z and Terashima K 2013 Self-organized pattern formation in helium dielectric barrier discharge cryoplasmas *Plasma Sources Sci. Technol.* **22** 025021
[11] Dong L, Shang J, He Y, Bai Z, Liu L and Fan W 2012 Collective vibration of discharge current filaments in a self-organized pattern within a dielectric barrier discharge *Phys. Rev.* E **85** 066403
[12] Stollenwerk L 2009 Interaction of current filaments in dielectric barrier discharges with relation to surface charge distributions *New J. Phys.* **11** 103034
[13] Bernecker B, Callegari T and Boeuf J P 2011 Evidence of a new form of self-organization in DBD plasmas: the quincunx structure *J. Phys. D: Appl. Phys.* **44** 262002

[14] Boeuf J P, Bernecker B, Callegari Th, Blanco S and Fournier R 2012 Generation, annihilation, dynamics and self-organized patterns of filaments in dielectric barrier discharge plasmas *Appl. Phys. Lett.* **100** 244108

[15] Zhang P and Kortshagen U 2006 Two-dimensional numerical study of atmospheric pressure glows in helium with impurities *J. Phys. D: Appl. Phys.* **39** 153

[16] Stollenwerk L, Amiranashvili Sh, Boeuf J-P and Purwins H-G 2006 Measurement and 3D simulation of self-organized filaments in a barrier discharge *Phys. Rev. Lett.* **96** 255001

[17] Bhoj A N and Kolobov V I 2011 Pattern formations in dielectric barrier discharges *Trans. Plasma Sci.* **39** 2152

[18] Xiong Z, Robert E, Sarron V, Pouvesle J-M and Kushner M J 2012 Dynamics of ionization wave splitting and merging of atmospheric-pressure plasmas in branched dielectric tubes and channels *J. Phys. D: Appl. Phys.* **45** 275201

[19] Babaeva N Yu and Kushner M J 2009 Effect of inhomogeneities on streamer propagation: I. Intersection with isolated bubbles and particles *Plasma Sources Sci. Technol.* **18** 035009

[20] Hirschberg J, Omairi T, Mertens N, Helmke A, Emmert S and Viol W 2013 Influence of excitation pulse duration of dielectric barrier discharges on biomedical applications *J. Phys. D: Appl. Phys.* **46** 154201

[21] Yang D-Z, Wang W-C, Zhang S, Tang K, Lieu Z-J and Wang S 2013 Multiple current peaks in room-temperature atmospheric pressure homogeneous dielectric barrier discharge plasmas excited by high-voltage tunable nanosecond pulse in air *Appl. Phys. Lett.* **102** 194102

[22] Liu C, Dobrynin D and Fridman A 2014 Uniform and non-uniform modes of nanosecond-pulsed dielectric barrier discharge in atmospheric air: fast imaging and spectroscopic measurements of electric fields *J. Phys. D: Appl. Phys.* **47** 252003